PHYSICAL REVIEW B VOLUME 24, NUMBER 6 15 SEPTEMBER 1981

Structural studies of graphite intercalation compounds using (00*l*) x-ray diffraction

S. Y. Leung* and M. S. Dresselhaus
Center for Materials Science and Engineering and Department of Electrical Engineering and Computer Science, Massachusetts Institute of Technology, Cambridge, Massachusetts 02139

C. Underhill†
Center for Materials Science and Engineering, Massachusetts Institute of Technology, Cambridge, Massachusetts 02139

T. Krapchev
Center for Materials Science and Engineering and Department of Materials Science and Engineering, Massachusetts Institute of Technology, Cambridge, Massachusetts 02139

G. Dresselhaus
Francis Bitter National Magnet Laboratory, Masschusetts Institute of Technology, Cambridge, Massachusetts 02139

B. J. Wuensch
Department of Materials Science and Engineering, Massachusetts Institute of Technology, Cambridge, Massachusetts 02139
(Received 10 February 1981)

Analysis of the (00*l*) x-ray diffractograms of graphite intercalation compounds reveals important structural information concerning these compounds. In particular, the in-plane intercalate density is observed to depart from the commonly accepted stoichiometric values. This result has important implications concerning various structural phase transformations that have been reported in these materials. The application of Fourier synthesis to the (00*l*) integrated intensities yields the projected structure of the intercalate layer onto the *c* axis. A least-squares refinement program RFINE4 was used to analyze the (00*l*) integrated intensities, yielding in-plane intercalate densities, Debye-Waller temperature factors, and various layer separations. The graphite-graphite layer separations were found to be not significantly different from the values for pristine graphite. Connections of the results of (00*l*) x-ray diffraction with other structural-analysis techniques such as electron diffraction and electron microscopy are discussed.

I. INTRODUCTION

The principal use of x-ray diffraction in the study of graphite intercalation compounds as been largely confined to stage identification.[1] There has been a moderate amount of work to extend the use of x-ray diffraction techniques to obtain other detailed structural information, and some examples of such work follow. Eeles and Turnbull[2] used (*hk*0) reflections on graphite-Br_2 to obtain information on in-plane ordering. Sasa *et al.*[3] extended the work of Eeles and Turnbull, utilizing (00*l*) integrated intensities to confirm that the in-plane stoichiometry of well-staged graphite-Br_2 samples is $C_{8n}Br_2$, where n is the stage index. Metz and Hohlwein[4,5] demonstrated that both the peak position and linewidth of the (00*l*) diffraction profile could be used to characterize the homogeneity and stage fidelity of the sample. They also showed that the diffractograms for a randomly staged sample could be explained by a one-dimensional disordered structure. Parry *et al.*,[6,7] utilizing the (*hk*0) diffraction lines for graphite-alkali-metal compounds, obtained information concerning the in-plane ordering, intercalate stacking, and in the case of graphite-K, also the in-plane carbon-carbon nearest-neighbor separation as a function of intercalate concentration. Parry's work was extended by Guérard *et al.*,[8] who correlated the change of in-plane graphite lattice constant with Z/r (where Z is the valence of the ion and r the ionic radius) for a large number of donor compounds. This

model[8] is difficult to interpret for acceptor compounds where both Z and r are not clearly defined. Flandrois *et al.*[9] have suggested a solution to this difficulty by correlating the change in the in-plane carbon-carbon distance with charge transfer which is determined by a separate experiment. They have been able to fit all reported results on the change in the in-plane carbon-carbon distance to a straight line where the abscissa (charge transfer) and the ordinate (change in the in-plane carbon-carbon distance) were determined independently. Hastings *et al.*[10] used the profile of x-ray powder peaks to obtain an estimate of the probability of c axis stacking faults in a stage-2 graphite-K compound. In this work, they defined a parameter α, the probability of finding a fault in going from one sandwich to another, and obtained a value of $\alpha = 0.38$. Zabel *et al.*,[11,12] Hastings *et al.*,[10] and Clarke *et al.*[13,14] used the (hkl) diffraction lines to study phase transformations in the graphite-K and graphite-Cs systems, following the initial work of Nixon and Parry.[15] Caswell *et al.*[16] used the extended x-ray absorption-fine-structure (EXAFS) technique to obtain information concerning the carbon-intercalant-carbon sandwich thickness d_s, and also the puckering distortion of the graphite-bounding layers. More recently, Wada *et al.*[17] used x-ray diffraction investigate a staging transition caused by the application of pressure on the stage-2 graphite-K system.

The first report of in-plane structure for a graphite—alkali-metal compound was made by Rüdorff.[18] Perfect stoichimetry, $C_{\xi n}X$, where n is the stage and in this case ξ is an integer (i.e., $\xi = 8$ for stage 1 and $\xi = 12$ for $n \geq 2$ graphite—alkali-metal compounds), has been assumed for these intercalation compounds by a large number of investigators since this early work. Evidence for departures from perfect stoichiometry comes from recent electron diffraction work by Kambe *et al.*[19–21] who showed coexistence of multiple intercalate phases in these compounds. They also found that different in-plane superlattices could exist at different parts of the same single-stage sample.

The preceding applications of x-ray diffraction to intercalation compounds have been specialized and fall considerably short of the full capability of diffraction analysis to provide coordinates and thermal vibration parameters for the three-dimensional arrangement of atoms within the unit cell of the intercalant. The nature of intercalated graphite has usually precluded analysis to the level normally permitted by these highly-developed techniques. The host material most commonly used to make graphite intercalation compounds is highly-oriented pyrolytic graphite (HOPG), a synthetic polycrystalline material with a crystallite size of about one micron within the graphite layers.[22] At best the c axes of the crystallites in HOPG are aligned to within 0.1° of each other, while the a axes within the layers are randomly oriented. The reciprocal-lattice points for general reflections (hkl) are accordingly distributed in rings about c, while the $(00l)$ reciprocal-lattice points, corresponding to diffraction from the layers, remain discrete points as in a single crystal.

The present work applies full crystallographic analysis to the information contained within the sharp $(00l)$ reflections produced by HOPG intercalates. The results are analogous to those which may be obtained through full three-dimensional analysis of a structure except that, as is well known, analysis of diffraction effects along a single direction in reciprocal space provides information on the projections of the structure onto the corresponding axis of the crystal. This limitation is not without some advantage in the study of intercalates since the presence of layer disorder and stacking faults will not influence the results. Many of the features of interest (for example, the spacing of the layers and the configuration and occupancy of the intercalated layers) can be obtained without ambiguity from analysis of the projected structure. Specifically, the present work is concerned with (1) the length of the c axis, and hence the stage, on the basis of either location of the $(00l)$ maxima, or the location of the maximum intensity within a derived "envelope function"; (2) the extent of stage infidelity through the intensity of maxima identified with the secondary stage; (3) stage inhomogeneity as determined by the half-widths of the $(00l)$ reflections; (4) the average in-plane intercalate density through a least-squares fit to measurement of the $(00l)$ integrated intensities; (5) the separations of graphite-graphite and graphite-intercalate layers through a least-squares fit of the projected atomic coordinates; (6) Fourier synthesis of the structure of molecular intercalants as projected onto the c axis; and (7) the c axis component of the mean-squared thermal displacement and the Debye-Waller factor.

The projected structures of a number of atomic and molecular intercalation compounds have been analyzed and are presented along with a summary of some preliminary work which has been previously reported.[23,24] The structures are generally found

to deviate from the assumed perfect stoichiometry. The implications of this result are discussed along with possible extensions.

II. EXPERIMENTAL DETAILS AND ANALYSIS

Samples were prepared in a two-zone furnace using graphite HOPG as the host material. Because of the instability of most of the samples in air, the crystals were encapsulated in pyrex ampoules with either a round or square cross section. The surface of the planar graphite sample was positioned as closely as possible across the diameter of a round ampoule or across the diagonal of the square ampoules.

The x-ray measurements were performed on a G.E. diffractometer using Mo $K\alpha$ radiation [$\lambda(K\alpha_1) = 0.709\,26$ Å, $\lambda(K\alpha_2) = 0.713\,54$ Å] to minimize absorption by the glass ampoule. Transmission through the ampoule was nevertheless only about 25%. The ampoule was mounted in a goniometer head to allow positioning of the surface of the graphite sample and alignment of the c axis in the plane of the incident and diffracted beams. Diffracted ($00l$) intensities were measured in a $\theta-2\theta$ scan using an Si(Li) drifted detector and a single-channel analyzer to separate the Mo $K\alpha$ peaks from the continuum. The same experimental arrangement could have been used to measure ($hk0$) reflections by rotating the crystal 90° and averaging around a diffraction ring (e.g., by spinning the sample[1]).

All diffraction patterns were recorded at room temperature. A number of representative ($00l$) diffractograms have already been published, including those obtained from graphite–alkali-metal compounds with K, Rb, and Cs (Refs. 23 and 25) as intercalants, for graphite-$FeCl_3$ compounds,[26] and for graphite-$AlCl_3$ compounds.[27]

The experimentally measured integrated intensities, I_{00l}, were converted to structure factors, F_{00l}, using the relation

$$I_{00l} = SC_L C_s C_g |F_{00l}|^2 , \tag{1}$$

where S is a scale factor and C_L is the combined Lorentz and polarization correction which, for an experiment in which radiation is normally incident on a rotation axis lying in the diffraction plane, takes the form $C_L = (1 + \cos^2 2\theta)/\sin 2\theta$. The correction for x-ray absorption by the planar graphite sample is $C_s = \exp(-2\mu t/\sin\theta)$, where μ and t are the linear absorption coefficient and thickness of the sample, respectively. The factor C_g is necessary to correct for absorption by the glass ampoule.[23] For the ampoules with square cross section

$$C_g = \exp[-2\mu_g d_g/\sin(\theta + \pi/4)] ,$$

where μ_g and d_g are, respectively, the linear absorption coefficient and wall thickness of the glass. In the case of a cylindrical ampoule $C_g \approx \exp(-2\mu_g d_g)$, and the angular dependence of the correction was neglected for the small range of angles pertinent to our measurements. Departure of the position of the graphite sample from its ideal location within the ampoule is a potential source of error in this correction. Several runs were made for each sample to ensure that such effects were minimal.

The structure factor F_{hkl} is given by the sum of the diffracted amplitudes contributed by each of the atoms in the unit cell.[28–30] When one considers ($00l$) reflections only, the structure factor reduces to the simpler form

$$F_{00l} = \sum_j f_j \exp(2\pi i l z_j) , \tag{2}$$

and contains information on the structure projected onto the c axis. Here z_j denotes the coordinates of the jth layer within the unit cell, the scattering factor for layer j is given by

$$f_j = f_j^0 \exp(-B_j \sin^2\theta/\lambda^2)$$
$$= f_j^0 \exp(-8\pi^2 \langle Z^2 \rangle \sin^2\theta/\lambda^2) ,$$

where f_j^0 is the scattering factor for the layer at rest, B_j is the Debye-Waller temperature factor, and $\langle Z^2 \rangle$ is the mean-squared thermal displacement of the layer normal to the diffracting planes.

As no information on the ordering or periodicity within the layers is available from ($00l$) data, we have found it convenient in this work to use a structure factor $\bar{F}$ defined as a *structure factor scaled to a single carbon atom per layer,* that is, $\bar{F} = F/\xi$, where ξ is the number of carbon atoms per layer in the cell of the intercalate. Moreover, it is reasonable to assume that the structure of the intercalate when projected onto the c axis is centrosymmetric about the intercalated layers. Upon selection of the origin at the intercalate layer denoted by X, Eq. (2) becomes, for even stages of a monatomic intercalant,

$$\bar{F}_{00l} = \frac{f_X}{\xi} + 2f_C \sum_{j=1}^{n/2} \cos(2\pi l z_j) , \tag{3}$$

and for odd stages

$$\bar{F}_{00l} = \frac{f_X}{\xi} + f_C \cos\pi l + 2f_C \sum_{j=1}^{(n-1)/2} \cos(2\pi l z_j) , \tag{4}$$

in which f_X and f_C refer to the intercalate and car-

bon layers, respectively. For polyatomic intercalants the intercalate layer will consist of an odd number of constitutive layers which will remain centrosymmetric upon projection. The scattering contribution f_X in Eqs. (3) and (4) may then be replaced by

$$f_X = f_{X_1} + 2\sum_{j=2}^{(n_X+1)/2} f_{X_j}\cos(2\pi l z_j) , \quad (5)$$

where n_X is the number of constituent intercalate layers (e.g., $n_X = 1$ for the alkali-metal compounds, but $n_X = 3$ for $FeCl_3$ or $NiCl_2$).

The stage of a given intercalation compound may be deduced from the length of c, the repeat distance in the z direction, as determined from the angular positions of the $(00l)$ maxima. The $(00l)$ intensity distribution specified by Eqs. (3) and (4) may also be used to this end in a qualitative fashion.[24] If $f_X \simeq f_C$, the trigonometric terms in Eqs. (3) and (4) define an envelope function for the intensity distribution whose utility lies in the fact that the relative intensities for all intercalants of a given stage can be related by a single plot. For intercalate layers of thickness comparable to the interlayer separation c_0 in graphite, the most intense $(00l)$ diffraction maxima occur for $l = n + 1$. In general, for intercalants with sandwich thickness d_s (the distance separating two graphite layers between which the intercalant is sandwiched), the maximum intensity occurs at $(00n + m)$, where m is the nearest integer which approximates $(d_s - c_0)/c_0$, where $c_0 = 3.35$ Å. Values of $m = 0$, 1, and 2 have been found for the intercalants Li, K, and $FeCl_3$, respectively.[31,23,26] The approximation is valid for intercalants with low atomic number, or for cases in which the number of intercalate atoms per cell is small compared with the number of carbon atoms. The l values for the reflection with maximum intensity may then be used as a rapid method for stage identification.

The least-squares structure refinement program RFINE4 (Ref. 32) was used to obtain precise values of the layer positions within the intercalate sandwich, the average occupancy of the intercalate layers, and the mean-squared thermal displacement along c by adjusting the values of the parameters in Eqs. (3) and (4) to provide a least-squares fit between the observed and calculated structure factors. The standard measures used to assess the agreement are the residual[29]

$$R = \sum \big| |F^{\text{obs}}| - |F^{\text{calc}}| \big| \Big/ \sum |F^{\text{obs}}| ,$$

or the weighted residual[33]

$$R_w = \left[\sum w(|F^{\text{obs}}| - |F^{\text{calc}}|)^2 \Big/ \sum w |F^{\text{obs}}|^2 \right]^{1/2} ,$$

where w is a weight defined for each observation in terms of the variance, σ^2, such that $w = \sigma^{-2}$. In normal structure analysis $R < 0.1$ indicates a satisfactory model and $R \approx 0.05$ a well-refined structural model.

Direct representations of the distribution of scattering density projected onto the c axis were obtained from the Fourier summation

$$\rho(z) = \frac{1}{c}\sum_{l=-\infty}^{\infty} F_{00l}\exp(-2\pi i l z) , \quad (6)$$

in which the unknown phases of F_{00l} were obtained from the model structure. As the phases are constrained to one of two values (0 or π for the centrosymmetric projections of this study), they are insensitive to small changes in the assumed structure. The summation could accordingly be evaluated in all instances without ambiguity.

III. RESULTS AND ANALYSIS

The use of $\theta-2\theta$ diffractograms for sample characterization is illustrated in Fig. 1 for graphite-$FeCl_3$ compounds. Secondary peaks indicating small admixtures of other stages are apparent in the diffractogram labeled as stage 1, where peaks due to pure graphite regions are found. The stage-3 sample shows small admixtures of stage 4, and the stage-4 sample shows small stage-3 regions. These spectra are in agreement with results found by other workers[4,5] showing that stage-1 graphite-$FeCl_3$ compounds of large size are very difficult to grow and almost always contain regions of pure graphite within the sample. It has been our observation that it is easier to grow single-stage compounds with $AlCl_3$, Br_2 and the alkali-metal intercalants[3,23,25,27] than with $FeCl_3$.

Evidence for stage homogeneity and stage fidelity other than the absence of secondary peaks in the diffractograms comes from the analysis of the full width at half maximum (FWHM) of the diffraction peak. Metz and Hohlwein[4,5] have shown that a random spacing between intercalate layers, shifts the position of the diffraction peaks and increases the FWHM of the corresponding peaks relative to the single-stage material. In Fig. 2 we have plotted the FWHM for HOPG, and for the stage-1 and -2 graphite—alkali-metal compounds in units of $\Delta(\sin\theta/\lambda)$ vs $\sin\theta/\lambda$. It can be seen from the figure

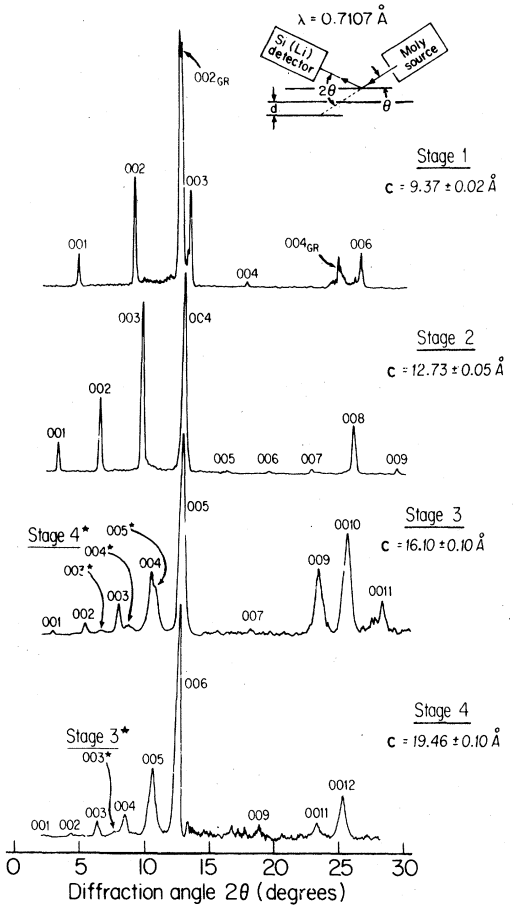

FIG. 1. X-ray stage characterization for stages $n = 1$, 2, 3, and 4 graphite-$FeCl_3$ compounds. The intercalate repeat distance c and stage indices are given on the right . Reflections due to admixed stages are indicated by ($00l^*$). The peaks labeled ($00l_{GR}$) in the stage-1 trace refer to the pristine graphite reflections.

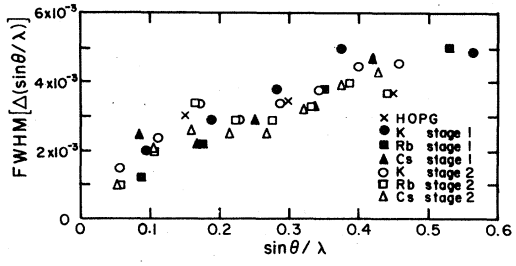

FIG. 2. Plot of the full width at half maximum (FWHM) of the ($00l$) diffraction lines in units of $\Delta(\sin\theta/\lambda)$ vs $\sin\theta/\lambda$ for stage-1 and -2 graphite–alkali-metal compounds and for HOPG. The diffractograms on which this analysis was made are given in Refs. 23 and 25.

that the FWHM of the reflections for the intercalation compounds is not significantly different from those for the parent material (HOPG). By comparing the FWHM of the intercalation compounds to that of pristine graphite (HOPG), one can conclude not only that the samples are single staged but also that there is little statistical disordering of the layers. Furthermore, according to Metz's model, stage 1 is a pure-stage compound. Since the FWHM points for our stage-2 compounds fall on top of the curve for that of the stage-1 compound, we conclude that our stage-2 compounds are also pure-stage compounds (i.e., not randomly staged). The results shown in Fig. 2 further point out that upon intercalation, the mosaic spread of the graphite intercalation compounds does not deviate much from that of pure graphite.

By analyzing the peak positions of the ($00l$) diffraction peaks we can obtain an accurate measurement of the unit-cell length c along the c axis, by making a chi-square, χ^2 minimization of $\Delta(2\theta_{l,l'}) = 2(\theta_l - \theta_{l'})$, the angular difference between each pair of ($00l$) and ($00l'$) diffraction lines . This difference technique is used to eliminate zero-point calibration errors.[34]

The structure of the intercalant layer can be obtained from the ($00l$) diffractometer scans using the analysis of Eqs. (1)–(5). As an example of the type of information that can be obtained, we have considered the internal layer structure of the intercalant in graphite-$AlCl_3$ with regard to whether it is the Al or the Cl layer that is adjacent to the graphite-bounding layer.[24] The ($00l$) integrated intensity measurements show a much better fit to Cl_3-Al_2-Cl_3 layers than to Al-Cl_6-Al layers.[24] Our best fit to the Cl_3-Al_2-Cl_3 structure is for the chemical formula $C_{9n}AlCl_3$ and an Al-Cl layer separation of ~ 1.40 Å, which is (within experimental error) in agreement with the chemical formulas $C_{8.4n}AlCl_3$ (Refs. 35 and 36) and $C_{9n}AlCl_3$ (Ref. 37) given in the literature. The Al-Cl layer separation found in the intercalation compound is also very close to the value of 1.35 Å for pristine $AlCl_3$.[38]

Further support for this identification of the sandwich structure of the $AlCl_3$ intercalant comes from a Fourier synthesis of the integrated intensities, and this approach is more quantitative than the model calculation of Ref. 24. Figure 3 shows the electron charge distribution as obtained from the Fourier synthesis of a stage-2 $AlCl_3$ compound using 11 ($00l$) diffraction lines. The figure is consistent with the assignment of the Al to the center of

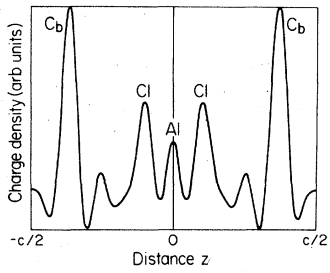

FIG. 3. Charge density along the c axis from a Fourier synthesis of the (00l) integrated intensities for 11 lines in a stage-2 graphite-$AlCl_3$ sample. The peaks labeled Al, Cl, and C_b represent the aluminum, chlorine, and graphite-bounding layers, respectively. Note the triple peak of the intercalant indicating a three layer intercalate structure. The diffractograms on which this analysis was made are given in Ref. 27.

the intercalant sandwich and the Cl in between the Al layer and the graphite-bounding layers C_b. This identification is made considering the relative heights of the peaks in the charge distribution, where in the ideal structure the Al layer has $13q$ electrons, the Cl layer $3 \times 17q = 51q$ electrons, and the graphite layer $9 \times 6q = 54q$ electrons, where q is the number of in-plane unit cells. From the location of the peaks of the charge distribution, one can directly measure the various layer separations in the intercalation compound. Such a tabulation for stages 1, 2, 4, and 8 graphite-$AlCl_3$ is given in Table I.

The small satellite peak adjacent to the strong maximum at the carbon location is a series-termination effect which arises form the finite number of terms (11) available for the Fourier summation of the charge distribution. In a one-dimensional summation, the distance from the atom location to the first maximum in the "Fourier ripple" about the image is $1.24d_{\min}(l_{\max})$, where $d_{\min}(l_{\max})$ is the minimum spacing of the Bragg planes for which a term is included in the summation.[39] The observed separation of the satellite form the carbon atom location in Fig. 3 is 3.67 Å, which is in excellent agreement with the expected value $1.24d_{\min}(11) = 3.71$ Å, thus confirming our interpretation of this peak. The one-dimensional nature of the summation makes termination effects especially pronounced in our synthesis of the charge density. The amplitude of the ripple increases, and the wavelength of the oscillation decreases as one moves from a three-dimensional to a one-dimensional summation of terms truncated at a given $d_{\min}(l_{\max})$.[39]

In Fig. 4, we show the c-axis charge density from the Fourier synthesis of the measured integrated intensities for stage-4 graphite-K, a compound having an atomic intercalant. In contrast to the results for graphite-$AlCl_3$, this figure shows a single peak centered on the intercalant and corresponding to the center of the graphite-intercalant-graphite sandwich. The peaks labeled C_b and C_i correspond to the graphite-bounding and interior layers, respectively, where the graphite-bounding layers are adjacent to the intercalant and the graphite interior layers are not. Application of the Fourier synthesis method to a molecular intercalant has also been carried out for a stage-4 graphite-Br_2 sample using the data of Sasa *et al.*,[3] and the results are shown in Fig. 5. The

TABLE I. Interplanar layer separations[a] in graphite-$AlCl_3$ from the peaks in the c-axis charge density obtained from the Fourier synthesis of the (00l) reflections.

Various interplanar layer separation (Å)	Stage index 1	2	3	4
c	9.49	12.91	19.67	32.88
d_s	9.49	9.52	9.60	9.34
d(Al-Cl)	1.47	1.30	1.44	1.32
$d(C_b - C_i)$		3.40[b]	3.35	3.36
$d(C_i - C_i)$			3.36	3.36

[a] c refers to the c-axis repeat distance and d_s refers to the graphite-intercalant-graphite sandwich thickness.

[b] For a stage-2 compound, $d(C_b - C_i)$ refers to the separation between the two adjacent graphite-bounding layers.

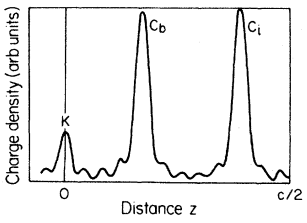

FIG. 4. Charge density along the c axis obtained from a Fourier synthesis of the (00l) integrated intensities for 23 lines in a stage-4 graphite-K sample. The peaks labeled K, C_b, and C_i denote maxima in the charge density associated with the potassium, graphite-bounding, and graphite interior layers, respectively. Note the single intercalate peak in contrast to the triple peaks in Fig. 3.

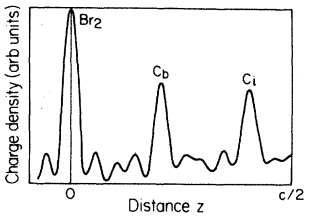

FIG. 5. Charge density along the c axis obtained from a Fourier synthesis of the (00l) integrated intensities for 21 lines in a stage-4 graphite-Br_2 sample. The peaks labeled Br_2, C_b, and C_i, respectively, denote maxima in the charge density associated with the bromine, graphite-bounding, and graphite interior layers. Note the single intercalate peak, indicating the co-planar structure of the Br_2 molecule in graphite-Br_2.

single peak at the center of the intercalant sandwich is consistent with the interpretation that the Br_2 molecule lies co-planar in the intercalate layer.[2]

Both Figs. 4 and 5 also display weak maxima associated with Fourier termination effects. The observed separation between a given atom location and the adjacent satellite again agrees well with the location computed from the minimum spacing which was employed in the synthesis: 0.70 Å as compared with $1.24d_{\min}(23) = 0.83$ Å for stage-4 graphite-K (see Fig. 4), and 0.95 Å, as compared with $1.24d_{\min}(21) = 1.01$ Å for stage-4-Br_2 (see Fig. 5).

To obtain more precise values for the structural parameters, we have analyzed the (00l) structure factors using the least-squares structure refinement program RFINE4.[32] The results of the analysis for the in-plane intercalate density, the fractional intercalate site occupation, the graphite-intercalant-graphite sandwich thickness, the graphite bounding-bounding or bounding-interior layer separations, the graphite interior-interior layer separations, and the Debye-Waller temperature factors are shown, respectively, in Tables II–VII for a number of graphite-alkali-metal compounds. In Table VIII, we have listed the weighted residual indices and the number of (00l) line used in the analysis.

The results for the reciprocal in-plane densities [ξ in Eqs. (3) and (4)] shown in Table II imply that the in-plane densities of the intercalation compounds are not consistent with the stoichimetry $C_{\xi n}X$ for a stage-n compound, in which ξ is an *integer*. The "accepted" values have been $\xi = 8$ for stage 1, and $\xi = 12$ for stage 2 and higher-stage graphite–alkali-metal compounds.[1] For stage-1 graphite-K, -Rb, and -Cs compounds, we obtain, respectively, $C_{6.88}K$, $C_{7.82}Rb$, and $C_{9.10}Cs$ instead of C_8X (see Table II). These results apply to the specific samples that we measured. In this connection it is believed that one can change the in-plane density by changing the growth and staging condi-

TABLE II. Reciprocal in-plane density (ξ) for graphite–alkali-metal donor and graphite-Br_2 acceptor compounds resulting from the RFINE4 analysis.[a]

Intercalant	Stage index 1	2	3	4	5
K	6.88 ± 0.11	9.84 ± 0.50		10.31 ± 0.67	
Rb	7.82 ± 0.03	11.72 ± 0.45		10.04 ± 0.40	
		9.90 ± 0.14			
Cs	9.10 ± 0.17	15.06 ± 0.70			
Br_2		7.3 ± 0.1	8.0 ± 0.2	7.0 ± 0.2	9.5 ± 0.3

[a] The in-plane density is given by $1/\xi$, and the (00l) intensity data used for the analysis for the graphite-Br_2 compounds were obtained from Ref. 3.

tions. It has been shown by Wada *et al.*[17,40] that the application of pressure can also change the in-plane density of graphite-alkali-metal compounds.

One can interpret the deviation from the accepted stoichiometry of the compounds in Table II by one of the two following explanations: (1) The compounds consist of a single in-plane structural phase but have a large vacancy or interstitial concentration. For this interpretation, our results imply a 16% and 2% interstitial concentration for the K and Rb compounds, respectively, and a 12% vacancy concentration for the Cs compound if the C_8X stoichiometry is assumed. Or (2) there is a multiphase coexistence within these compounds (e.g., the K compound can have coexisting regions with C_6K and C_8K superlattices and discommensuration regions between them). Using the current interpretation of electron diffraction experiments,[19–21,41] the evidence seems to indicate that the multiphase coexistence explanation is more probable. Furthermore, Evans and Thomas[42] have reported both the C_6K and the C_8K superlattices for a stage-1 graphite-K compound. Kambe *et al.*[19–21] have also observed different superlattices in different portions of the same samples of low-stage alkali-metal compounds.

The in-plane densities for stage 2 and for higher stage compounds also show deviations from the accepted $C_{12n}X$ stoichiometry. For example, for the case of stage-2 graphite-Rb, there seems to be evidence for sample dependence of the in-plane densities which would indicate that growth conditions significantly alter the in-plane density. If an incommensurate intercalate ordering or only short-range intercalate correlations are assumed for the stage-2 alkali-metal compounds at room temperature, the site occupation should scale as the ratio of the square of the ionic radii $(r^2_{K^+}:r^2_{Rb^+}:r^2_{Cs^+})$ $=(1.00:1.22:1.61)$. Our results show that the fractional site occupation for K:Rb:Cs is in the ratio (1.00:1.19:1.53) so that an incommensurate in-plane structure or a disordered structure with only short-range correlations for the stage-2 graphite-alkali-metal compounds cannot be ruled out on the basis of the $(00l)$ integrated intensity measurements of Table II. One further point of interest is that the stage-4 graphite-K and graphite-Rb compounds follow the same general trend as the stage-2 compounds with regard to the in-plane densities, but the correlation of the fractional intercalate site occupation to the ionic radii cannot be made.

It is to be stressed that the values obtained for the in-plane densities are for the specific set of single-stage samples that were used in the present studies. Furthermore, the results only apply to the well-staged portions of the sample which contribute to

TABLE III. Fractional intercalate site occupation (ν) for several possible commensurate orderings for the graphite–alkali-metal compounds used in this study.

Stage	Chemical[a] formula	Superlattice[b]	ν(K)	ν(Rb)	ν(Cs)
1	C_6X_ν	$p(\sqrt{3}\times\sqrt{3})R30°$	0.87	0.77	0.66
1	C_8X_ν	$p(2\times 2)$	1.16	1.02	0.88
1	$C_{18}X_{2\nu}$	$h(3\times 3)$	1.31	1.15	0.99
2	$C_{36}X_{2\nu}$	$h(3\times 3)$	0.91	0.77[c]	0.66
				0.91[c]	
2	$C_{48}X_{2\nu}$	$h(\sqrt{12}\times\sqrt{12})R30°$	1.22	1.02[c]	0.80
				1.21[c]	
2	$C_{28}X_\nu$	$p(\sqrt{7}\times\sqrt{7})R19.1°$	1.42	1.19[c]	0.93
				1.41[c]	
4	$C_{72}X_{2\nu}$	$h(3\times 3)$	0.87	0.90	
4	$C_{96}X_{2\nu}$	$h(\sqrt{12}\times\sqrt{12})R30°$	1.16	1.20	
4	$C_{56}X_\nu$	$p(\sqrt{7}\times\sqrt{7})R19.1°$	1.36	1.39	

[a] The primitive superlattice has one X atom/unit cell (hence X_ν in the chemical formula) and the honeycomb superlattice has two X atom/unit cell (hence $X_{2\nu}$ in the chemical formula).
[b] The primitive and honeycomb hexagonal in-plane unit cells are specified by p and h, respectively.
[c] Two different values for ν are listed for Rb stage 2 because of the different in-plane densities found for the two samples in Table II.

the (00l) diffraction lines that are used in the analysis. If the intercalate material is preferentially located in grain boundaries, surfaces, etc., it does not give a coherent contribution to the (00l) lines and thus will not be included in this characterization method. An analysis based on the (00l) diffraction lines will not give information concerning the in-plane intercalate structure, which must be deduced from other techniques such as electron diffraction or (hkl) x-ray diffraction lines. In Table III, we have listed the fractional intercalate site occupation factor ν for several possible commensurate orderings *if* a pure phase is assumed for the intercalate layer.

Other information that can be obtained from the analysis of the (00l) reflection lines using RFINE4 is the Debye-Waller temperature factors for the Z displacement, which are tabulated in Table IV. The temperature factors must be interpreted with caution since no correction for the x-ray absorption by the glass ampoule was made for the case of round ampoules, and the temperature factor will absorb any systematic angular-dependent errors. However, for the case of the stage-1 graphite—alkali-metal compounds, the results are consistent and significant, insofar as the temperature factor of the alkali-metal decreases as a function of intercalant mass in the ratio (1.00: 0.50: 0.05). The temperature factor for each material is expected to scale with its inverse mass, and the ratio of the inverse masses for K:Rb:Cs is (1.00: 0.46: 0.29). While the Debye-Waller temperature factors for K and Rb scale like the inverse mass ratio, the behavior for Cs is anomalous and is about a factor of six too small. Furthermore, the temperature factors for the carbon atoms in the stage-1 compounds are fairly constant within experimental error. On the basis of the Debye-Waller temperature factors, we can compute the mean-square displacement $\langle Z^2 \rangle$ (in Å^2) and we obtain for our stage-1 graphite-alkali-metal compounds the following values:

$$\begin{aligned} \langle Z^2 \rangle_{\mathrm{K}} &= 0.0416 \pm 0.0076 , \\ \langle Z^2 \rangle_{\mathrm{Rb}} &= 0.0208 \pm 0.0010 , \\ \langle Z^2 \rangle_{\mathrm{Cs}} &= 0.0019 \pm 0.0037 , \\ \langle Z^2 \rangle_{\mathrm{C}} &= 0.0124 \pm 0.0085 . \end{aligned} \tag{7}$$

TABLE IV. Debye-Waller temperature coefficients B for the Z displacement of the intercalant (B_X), graphite-bounding layers (B_{C_b}), and graphite-interior layers (B_{C_i}), obtained from analysis of the (00l) reflection lines in graphite—alkali-metal donor compounds and the graphite-bromine acceptor compounds using RFINE4.

Intercalant	Stage	B_X	B_{C_b}	B_{C_i}
K	1	3.24 ± 0.60	0.81 ± 0.26	
Rb[a]	1	1.62 ± 0.08	0.99 ± 0.09	
Cs	1	0.15 ± 0.29	0.87 ± 0.61	
K	2	4.68 ± 2.04	3.98 ± 0.55	
Rb	2	6.02 ± 1.76	2.89 ± 0.80	
Rb	2	5.25 ± 0.61	1.17 ± 0.31	
Cs	2	-3.44 ± 1.05[b]	-3.04 ± 0.91[b]	
K	4	4.67 ± 2.74	0.51 ± 0.36	0.34 ± 0.35
Rb	4	2.08 ± 1.42	-0.28 ± 0.57[b]	-0.68 ± 0.49[b]
Br_2	2	1.19 ± 0.40	-0.25 ± 0.56[b]	
Br_2	3	1.02 ± 0.30	0.44 ± 0.51	0.99 ± 0.82
Br_2	4	0.26 ± 0.35	-1.17 ± 0.58[b]	-0.81 ± 0.51[b]
Br_2	5	0.17 ± 0.37	-0.48 ± 0.50[b]	-0.11 ± 0.49[b]
				-0.75 ± 0.63[b]

[a] For Rb stage 1 there is a large correlation between B_X and B_{C_b}, which are therefore minimized separately.

[b] Negative temperature coefficients for B_X, B_{C_b}, and B_{C_i} are not physical and may be related to an improper correction for the absorption by the glass ampoule.

TABLE V. Graphite-intercalant-graphite sandwich thickness (d_s) values in Å from analysis of the (00*l*) reflection lines in graphite—alkali-metal donor compounds and graphite-Br_2 acceptor compounds using RFINE4.

Intercalant	Stage 1	2	3	4	5
K	5.32 ± 0.02	5.38 ± 0.02		5.40 ± 0.04	
Rb	5.65 ± 0.01	5.66 ± 0.01[a]		5.72 ± 0.05	
		5.72 ± 0.01[a]			
Cs	5.95 ± 0.01	6.02 ± 0.02			
Br_2		7.00 ± 0.02	7.02 ± 0.02	7.02 ± 0.03	7.01 ± 0.02

[a] Results obtained for two different stage-2 graphite-Rb samples.

Values for the mean-square *c*-axis displacements $\langle Z^2 \rangle$ and for the Debye temperature corresponding to these displacements $\Theta_\perp$ (in K) have been reported for carbon and cesium atom displacement at 4.2 K in C_8Cs by Campbell *et al.*[43] using Mössbauer spectroscopy techniques, yielding

$$\langle \Theta_\perp \rangle_C = 800 \ , \qquad \langle Z^2 \rangle_C = 0.003\,76 \ , \tag{8}$$

and

$$\langle \Theta_\perp \rangle_{Cs} = 145 \ , \qquad \langle Z^2 \rangle_{Cs} = 0.001\,89 \ , \tag{9}$$

for the carbon and Cs atoms, which we extrapolate to room temperature (300 K) by the formula[44]

$$\langle Z^2 \rangle = \frac{3\hbar^2}{Mk_B\Theta_\perp}\left[\frac{1}{4} + \left[\frac{T}{\Theta_\perp}\right]^2 \int_0^{\Theta_\perp/T} \frac{x\,dx}{e^x - 1}\right] \tag{10}$$

to obtain

$$\langle Z^2 \rangle_{Cs} = 0.0157 \ , \qquad \langle Z^2 \rangle_C = 0.0067 \ . \tag{11}$$

The extrapolated value for $\langle Z^2 \rangle_{Cs}$ is about one order of magnitude greater than our value for $\langle Z^2 \rangle_{Cs}$ which we noted above is anomalously small. The extrapolated value for $\langle Z^2 \rangle_C$, on the other hand, within the error of our value for $\langle Z^2 \rangle_C$.

TABLE VI. Graphite-graphite interplanar layer separation[a] values in Å resulting from analysis of (00*l*) reflection lines in graphite—alkali-metal donor compounds and graphite-Br_2 acceptor compounds using RFINE4.

Intercalant	Stage 2	3	4	5
K	3.36 ± 0.02		3.34 ± 0.02	
Rb	3.39 ± 0.01		3.34 ± 0.03	
	3.34 ± 0.01			
Cs	3.34 ± 0.02			
Br_2	3.39 ± 0.02	3.36 ± 0.02	3.36 ± 0.02	3.39 ± 0.02

[a] For stage-2 compounds, the graphite-graphite interplanar layer separation is the distance between two adjacent bounding layers $d(C_b - C_b)$ not across the intercalant. For stage 3 and higher, the distance is the graphite bounding-interior layer separation $d(C_b - C_i)$.

Ellenson *et al.*[45] have measured the acoustic branch of the phonon spectrum for C_8Rb with neutron diffraction. Extrapolation of their result gives a value of $v_l = 3.61 \times 10^5$ cm/sec for the velocity of sound propagating in the z direction at room temperature (290 K). One can relate the velocity of sound v_l to the Debye temperature $\Theta_\perp$ if we assume that the velocity of sound is not temperature dependent. At low temperature, the relation between v_l and $\Theta_\perp$ takes the form[44]

$$\Theta_\perp = \frac{\hbar v_l}{k_B}\left[\frac{6\pi^2 N}{V}\right]^{1/3} . \tag{12}$$

A rough estimate for $(\Theta_\perp)_{Rb}$ can be made if we assume that N is the number of intercalate atoms per unit cell and V the volume of the unit cell. We thus obtain value of 219 K for $(\Theta_\perp)_{Rb}$ in C_8Rb. We note that the determination of the Debye temperature from specific-heat measurements gives an average over the contributions for the longitudinal and transverse velocities of sound, and because of the highly anisotropic nature of graphite, $\Theta_\perp$ cannot be obtained from specific-heat data unless both v_l and v_t are known. Using Eq. (10) we obtain, respectively, the zero-temperature and room-temperature mean-square displacement (in Å^2) as

$$\begin{aligned} \langle Z^2\rangle_{Rb}(T = 0\ \text{K}) &= 0.001\,94\ , \\ \langle Z^2\rangle_{Rb}(T = 300\ \text{K}) &= 0.010\,8\ . \end{aligned} \tag{13}$$

The room-temperature value is about a factor of 2 smaller than our value, but is considered to be consistent (within experimental error) with our result, in light of the approximations used to get $\Theta_\perp$.

TABLE VII. Values for graphite interior-interior layer separation $d(C_i - C_i)$ in Å resulting from analysis of the $(00l)$ reflection lines for several compounds using RFINE4.

Intercalant	Stage 4	Stage 5
K	3.35 ± 0.03	
Rb	3.36 ± 0.04	
Br_2	3.35 ± 0.03	3.31 ± 0.02

The interpretation of results for the Debye-Waller temperature coefficients for the higher stage alkali-metal compounds is more difficult in that these materials have no single definitive in-plane structure, and that in some cases the temperature factor even goes negative, which is an unphysical result. Unphysical Debye-Waller temperature coefficients were also obtained for some of the graphite-Br_2 compounds in Table IV.

Tabulated in Tables V, VI, and VII are the various layer separations that were obtained for the graphite-alkali-metal compounds and graphite-Br_2 compounds in this work. In Table V are listed values for the graphite-intercalant-graphite sandwich thickness d_s obtained RFINE4, showing an increase in d_s with increasing stage index for donor compounds. The bonding of the intercalate to the

TABLE VIII. Weighted residual index R_w obtained by analysis of $(00l)$ reflection lines using RFINE4.

Intercalant	Stage	R_w	Number of $(00l)$ lines
K	1	0.018	6
Rb	1	0.006	8
Cs	1	0.047	8
K	2	0.047	8
Rb	2	0.057	7
Rb	2	0.023	7
Cs	2	0.077	7
K	4	0.077	23
Rb	4	0.157	23
Br_2	2	0.072	12
Br_2	3	0.075	17
Br_2	4	0.099	21
Br_2	5	0.082	25

TABLE IX. Fit of observed and calculated (00l) structure factors for a stage-4 graphite-K sample using RFINE4. The in-plane density corresponds to $C_{10.3}K$. The residual is $R = 0.108$ and the weighted residual is $R_w = 0.077$ (see Table VIII).

l	$\lvert F_{00l}^{\text{expt}} \rvert$	$\lvert F_{00l}^{\text{calc}} \rvert$
1	97	95.6
2	117	123.8
3	179	185.0
4	470	474.9
5	693	714.6
6	182	180.8
7	67	75.4
8	9	9.3
9	487	411.8
10	266	213.4
11	147	129.5
12	124	105.0
13	148	137.4
14	307	290.3
15	21	13.0
16	57	41.3
17	70	59.2
18	187	209.8
19	125	166.2
20	38	52.7
23	144	210.5

TABLE X. Fit of observed and calculated (00l) structure factors for a stage-4 graphite-Br_2 compound using REFINE4. The in-plane density corresponds to $C_{14.4}Br_2$. The residual is $R = 0.154$ and the weighted residual is $R_w = 0.099$ (see Table VIII).

l	$\lvert F_{00l}^{\text{expt}} \rvert$	$\lvert F_{00l}^{\text{calc}} \rvert$
1	0[a]	56.5
2	60	61.7
3	64	69.7
4	112	90.9
5	399	420.8
6	52	35.7
7	68	61.0
8	80	74.4
9	80	99.5
10	291	279.6
11	16	26.0
12	32	54.7
13	80	68.5
14	116	94.5
15	255	216.9
16	0[a]	4.8
17	40	39.7
18	44	57.5
19	72	89.3
20	179	189.4
21	28	26.7

[a] No line was observed above the noise level.

graphite-bounding layer is expected to weaken the bond between the graphite-bounding layer and the interior layers. Thus the d_s value is smaller in the low-stage alkali compounds, where the higher intercalate density gives the strongest intercalate-graphite bonding (see Table V), in agreement with previous work, which was based on assuming stage independence for the graphite-graphite interplanar layer separation.[1,46] Evidence in support of the validity of this assumption is given in Table VI, where values are listed for the graphite-bounding–graphite-interior $d(C_b - C_i)$ interplanar layer separation based on RFINE4, and in Table VII, where the corresponding values for the $C_i - C_i$ layer separations are given. A determination of these graphite-graphite interplanar layer separations is also provided by EXAFS measurements on the graphite-alkali-metal compounds,[16] and their results are in agreement with the present work to within experimental error.

To evaluate the goodness of fit of the model to the experimental results, we list in Table VIII the residual indices obtained from the RFINE4 analysis. The lower the value for the residual R_w, the better the fit to the experimental data. A comparison of the experimental structure factor to the best fit to the data is shown in Tables IX and X, respectively, for a stage-4 graphite-K donor compound ($R_w = 0.077$) and a stage-4 graphite-Br_2 acceptor compound ($R_w = 0.131$). The good fit in Tables IX and X is indicative of a homogeneous sample.

The Hamilton significant test is applied to our model fit to test the significance of the various distance parameters used in fitting our result. The Hamilton significant test is a linear hypothesis test that relates the change of the weighted residual index to the addition of parameters in the model.[33,47] The result of the test for stage-2 and stage-4 graphite-alkali-metal compounds with respect to the addition of a parameter for the graphite-graphite interplanar layer separation is shown in Table XI. The application of the Hamilton significant test indicates that the graphite-graphite layer separation does not significantly deviate from 3.35 Å when these separations are treated as adjustable parameters. The results of Table XI show that the parameter α in all cases is found to be about 0.5, which means it

TABLE XI. The Hamilton significant test of the significance of including the interplanar layer separations as parameters in RFINE4. The definitions of p as "the addition of the new distance parameter," and $\bar{R} = R_w(\text{without } p)/R_w(\text{with } p)$ are given in the text.

Intercalant	K	Rb	Cs	K	Rb
Stage	2	2	2	4	4
Number of lines (q)	8	7	7	23	23
Number of lines (m)	5	5	5	7	7
R_w(with p)	0.047	0.057	0.077	0.077	0.157
R_w(without p)	0.047	0.071	0.077	0.078	0.162
$\bar{R}$	1.0	1.25	1.0	1.013	1.032
Number of distance parameters (b)	1	1	1	2	2
Degrees of freedom ($q-m$)	3	2	2	16	16
Significance level (α)	0.5	0.5	0.5	0.5	0.5
$\bar{R}_{b,q-m,\alpha}$	1.093	1.155	1.155	1.044	1.044

is equally probable that the distances are as calculated or that they remain unchanged relative to their pristine graphite unadjusted values.

We have also fit our data using an ionic scattering factor for the alkali metal in the graphite-alkali-metal compounds. This fitting gives no significant reduction of the residual index or changes in the values of the other parameters. This distinction between atomic and ionic scattering factors could be especially important in the stage-1 graphite-alkali-metal compounds because of the possibility of using x-ray diffraction measurements to test whether or not there is complete ionization of the alkali metal in the intercalate layer. The results for the ionic scattering factors are shown in Table XII. As we can see, the fit is insensitive to whether one uses an atomic or an ionic scattering factor for the analysis.

The inclusion of puckering of the graphite-bounding layer as an additional parameter was also considered. Our analysis shows that the inclusion of puckering of the graphite-bounding layers by as much as 0.5 Å does not give any statistically different results to the fit. Such a puckering effect for one of our phases would also have given rise to an anomalously large apparent Debye-Waller factor for the projected layers, if one had assumed planar sheets. This effect was not observed.

TABLE XII. Comparison between the use of atomic and ionic alkali-metal scattering factor for determination of the fractional intercalate site-occupation values (ν in C_8X_ν) for various stage-1 graphite—alkali-metal scattering factors in terms of the weighted residual R_w.

Atomic or ionic species	ν	R_w
K	1.162 ± 0.019	0.018
K^+	1.166 ± 0.019	0.018
Rb	1.023 ± 0.003	0.006
Rb^+	1.024 ± 0.003	0.006
Cs	0.879 ± 0.017	0.047
Cs^+	0.880 ± 0.017	0.047

IV. CONCLUSIONS

In this paper, we have obtained structural information on staging, in-plane densities, structure of the molecular intercalant, and various layer separations from analysis of the measured angular positions, linewidths, and integrated intensities of (00l) reflections. The results are significant in that we have found that the in-plane densities deviate from accepted stoichiometries and this conclusion is consistent with the interpretation of multiphase coexistence of different in-plane superlattice structures. Furthermore, we can determine the layer structure of molecular intercalants such as in graphite-$AlCl_3$ and graphite-Br_2 by calculating the c-axis dependence of the charge density using the Fourier synthesis method. A full structural determination of a single-crystal intercalation compound using many (hkl) lines remains a major goal for a definitive x-ray study. The in-plane density and lattice constants can be useful parameters to monitor structural transitions. Thus temperature-dependent x-ray measurements could provide a useful tool for extracting further structural information on these compounds. A key experiment suggested by the present work is the correlation of the in-plane intercalate

density with the growth conditions of the intercalation compounds.

ACKNOWLEDGMENTS

We wish to thank Dr. H. Mazurek and Professor R. Ogilvie for helpful discussions and Dr. A. W. Moore of Union Carbide for his generous contribution of the HOPG material. We gratefully acknowledge support for this work from NSF Grant No. DMR-78-10858. The Francis Bitter National Magnet Laboratory is supported by the National Science Foundation.

*Present address: Bell Telephone Laboratories, Murray Hill, N.J.

†Present address: Raytheon Laboratories, Waltham, Mass.

[1]A. Hérold, in *Physics and Chemistry of Materials with Layered Structures,* edited by F. Lévy (Reidel, Dordrecht, Holland, 1979), Vol. 6, p. 323.

[2]W. T. Eeles and J. A. Turnbull, Proc. R. Soc. London A283, 179 (1965).

[3]T. Sasa, T. Takahashi, and T. Mukaibo, Carbon 9, 407 (1971).

[4]W. Metz and D. Hohlwein, Carbon 13, 87 (1975).

[5]D. Hohlwein and W. Metz, Z. Kristallogr. 139, 279 (1974).

[6]D. E. Nixon and G. S. Parry, J. Phys. C 2, 1732 (1969).

[7]G. S. Parry, Mater. Sci. Eng. 31, 99 (1977).

[8]D. Guérard, C. Zeller, and A. Hérold, C. R. Acad. Sci. (Paris) C283, 437 (1976).

[9]S. Flandrois, J. Masson, J. Rouillon, J. Gaultier, and C. Hauw, Synthetic Met. 3, 1 (1981).

[10]J. B. Hastings, W. E. Ellenson, and J. E. Fischer, Phys. Rev. Lett. 42, 1552 (1979).

[11]H. Zabel, S. C. Moss, N. Caswell, and S. A. Solin, Phys. Rev. Lett. 43, 2022 (1979).

[12]H. Zabel, Y. M. Jan, and S. C. Moss, Physica (Utrecht) 99B, 453 (1980).

[13]R. Clarke, N. Caswell, and S. A. Solin, Phys. Rev. Lett. 42, 61 (1979).

[14]R. Clarke, N. Caswell, S. A. Solin, and P. M. Horn, Phys. Rev. Lett. 43, 2018 (1979).

[15]D. E. Nixon and G. S. Parry, J. Phys. D 1, 291 (1968).

[16]N. Caswell, S. A. Solin, T. M. Hayes, and S. J. Hunter, Physica (Utrecht) 99B, 463 (1980).

[17]N. Wada, R. Clarke, and S. A. Solin, Synthetic Met. 2, 27 (1980).

[18]W. Rüdorff and E. Schulze, Z. Anorg. Allg. Chem. 277, 156 (1954).

[19]N. Kambe, G. Dresselhaus, and M. S. Dresselhaus, Phys. Rev. B 21, 3491 (1980).

[20]M. S. Dresselhaus, N. Kambe, A. N. Berker, and G. Dresselhaus, Synthetic Met. 2, 121 (1980).

[21]N, Kambe, G. Dresselhaus, M. S. Dresselhaus, and A. N. Berker, Physica (Utrecht) 105B, 272 (1981).

[22]A. W. Moore, in *Chemistry and Physics of Carbon,* edited by P. L. Walker and P. A. Thrower (Dekker, New York, 1973), Vol. 11, p. 69.

[23]S. Y. Leung, C. Underhill, G. Dresselhaus, T. Krapchev, R. Ogilvie, and M. S. Dresselhaus, Solid State Commun. 32, 635 (1979).

[24]S. Y. Leung, C. Underhill, G. Dresselhaus, T. Krapchev, R. Ogilvie, and M. S. Dresselhaus, Phys. Lett. 76A, 89 (1980).

[25]S. Y. Leung, C. Underhill, G. Dresselhaus, and M. S. Dresselhaus, Solid State Commun. 33, 285 (1980).

[26]C. Underhill, S. Y. Leung, G. Dresselhaus, and M. S. Dresselhaus, Solid State Commun. 29, 769 (1979).

[27]G. M. Gualberto, C. Underhill, S. Y. Leung, and G. Dresselhaus, Phys. Rev. B 21, 862 (1980).

[28]B. D. Cullity, *Elements of X-ray Diffraction* (Addison-Wesley, Reading, Massachusetts, 1956).

[29]*International Tables for X-ray Crystallography,* edited by J. A. Ibers and W. C. Hamilton (Kynock, Birmingham, England, 1974), Vol. 4.

[30]C. Kittel, *Introduction to Solid State Physics,* 4th ed. (Wiley, New York, 1971).

[31]S. Basu, C. Zeller, P. Flanders, C. J. Fuerst, W.D. Johnson, and J. E. Fischer, Mater. Sci. Eng. 38, 275 (1979).

[32]L. W. Finger and E. Prince, NBS Technical Note 854 (unpublished).

[33]W. C. Hamilton, Acta Crystallogr. 18, 502 (1965).

[34]S. Y. Leung, ScD. thesis, MIT, Cambridge, Mass., 1980 (unpublished).

[35]W. Rüdorff and R. Zeller, Z. Anorg. Allg. Chem. 279, 182 (1955).

[36]J. G. Hooley, *Preparation and Crystal Growth of Materials with Layered Structures,* edited by R.M.A. Lieth (Reidel, Dordrecht, Holland, 1977), Vol. 1, p. 1.

[37]E. Stumpp, Mater. Sci. Eng. 31, 53 (1977).

[38]R. W. G. Wyckoff, *Crystal Structures* (Interscience, New York, 1964).

[39]R. W. James, Acta Crystallogr. 1, 132 (1948).

[40]N. Wada, (unpublished).

[41]A. N. Berker, N. Kambe, G. Dresselhaus, and M. S. Dresselhaus, Phys. Rev. Lett. 45, 1452 (1980).

[42]E. L. Evans and J. M. Thomas, J. Solid State Chem. 14, 99 (1975).

[43]L. E. Campbell, G. L. Montet, and G. J. Perlow, Phys. Rev. B 15, 3313 (1977).

[44]C. Kittel, *Quantum Theory of Solids* (Wiley, New, York, 1963).

[45]W. D. Ellenson, D. Semmingsen, D. Guérard, D. G. Onn, and J. E. Fischer, Mater. Sci. Eng. 31, 137 (1977).

[46]M. S. Dresselhaus and G. Dresselhaus, Ad. Phys. 30, 139 (1981).

[47]W. C. Hamilton, *Statistics in Physical Science; Estimation, Hypothesis Testing and Least Squares* (Ronald Press, New York, 1964).